

## Tidal current-induced formation——storm-induced change——tidal current-induced recovery\*

——Interpretation of depositional dynamics of formation and evolution of radial sand ridges on the Yellow Sea seafloor

ZHANG Changkuan (张长宽), ZHANG Dongsheng (张东生),

ZHANG Junlun (张君伦) and WANG Zhen (王震)

(Hehai University, Nanjing 210098, China)

Received February 26, 1998

**Abstract** The results of simulated tidal current field, wave field and storm-induced current field are employed to interpret the depositional dynamic mechanism of formation and evolution of the radial sand ridges on the Yellow Sea seafloor. The anticlockwise rotary tidal wave to the south of Shandong Peninsula meets the following progressive tidal wave from the South Yellow Sea, forming a radial current field outside Jianguang. This current field provides a necessary dynamic condition for the formation and existence of the radial sand ridges on the Yellow Sea seafloor. The results of simulated "old current field (holocene)" show that there existed a convergent-divergent tidal zone just outside the palaeo-Yangtze River estuary where a palaeo-underwater accumulation was developed. The calculated results from wave models indicate that the wave impact on the topography, under the condition of high water level and strong winds, is significant. The storm current induced by typhoons landing in the Yangtze River estuary and turning away to the sea can have an obvious influence, too, on the sand ridges. The depositional dynamic mechanism of formation and evolution of the radial sand ridges on the Yellow Sea seafloor is "tidal current-induced formation——storm-induced change——tidal current-induced recovery".

**Keywords:** depositional dynamics, radial sand ridges on the Yellow Sea seafloor, tidal current sand ridges, South Yellow Sea, storm current field.

Radial sand ridges on the Yellow Sea seafloor are distributed over the middle part of Jiangsu coast down from the Yangtze River estuary up to the Sheyang estuary, stretching for 200 km latitudinally and 90 km longitudinally. There are more than 70 sand ridges radiating from Jianguang (see fig. 1), most of which come out of water and become shoals at low water level. These sand ridges are of different heights and in different shapes, and form a peculiar geomorphology, which is unique in the world. For such huge sand ridges, during the period of their formation, development, evolution and maintenance, there must exist a special and relatively stable dynamic environment. Therefore, the study on the dynamic conditions of the sand ridges and the depositional dynamic mechanism of the formation and evolution of radial sand ridges is one of the important parts of the study on the sand ridges on the Yellow Sea seafloor.

Because of the lack of the measured oceanographic data and the significant influence of the complicated local seabed topography on the field data, the numerical results of the tidal current field, the wave field and the storm induced current field are employed to interpret the depositional dynamic mechanism for the formation and evolution of the radial sand ridges on the Yellow Sea seafloor.

\* Project supported by the National Natural Science Foundation of China (Grant No. 49236120).

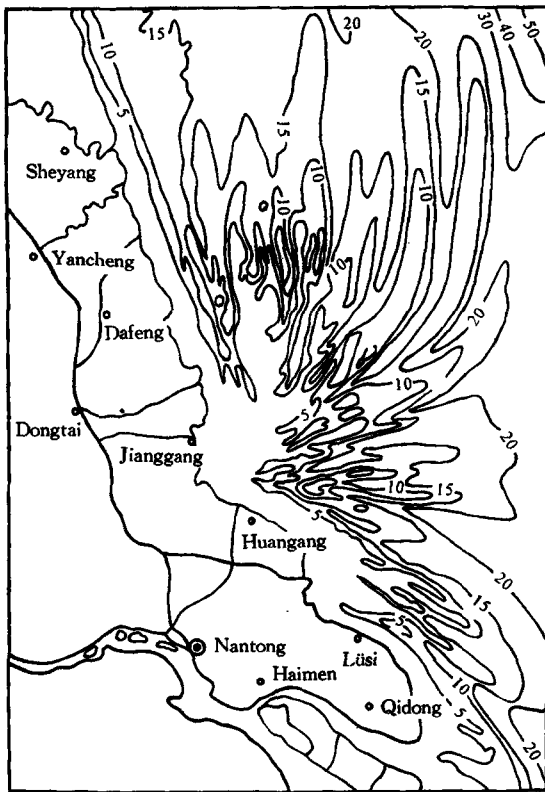


Fig. 1. Radial sand ridges on the Yellow Sea seafloor.

hydraulic conditions for the formation of sand ridge bases? Thirdly, during the long period of evolution of sand ridges, does the tidal wave system change?

### 1.1 Present current field and radial plane form of sand ridges

For different purposes, many researchers carried out numerical simulations of the tidal current over the East China Sea, and suggested that there existed a convergent tidal zone along Jiangsu coast of the South Yellow Sea<sup>[5,6]</sup>. However, those arguments are far from enough to answer the above three questions. Therefore, numerical investigation of the semidiurnal constituent,  $M_2$ , over the sand ridges of the South Yellow Sea is conducted. Tidal wave distributions and tidal current fields both at present and in the past are simulated<sup>[7]</sup>.

“The present tidal current field” is a brevity, and means that the current field is calculated by use of the present coast line as land boundary in the numerical model. The present tidal current field of constituent  $M_2$  is unique. After entering the South Yellow Sea, some of the constituent  $M_2$  pass by the Shandong Peninsula and continue their way, and the rest are stopped by the peninsula and form anticlockwise rotary tidal wave to the south of the peninsula. This rotary wave meets the following progressive tidal wave from the South Yellow Sea, forming stationary tidal wave. This wave is named moving stationary tidal wave. Influenced by bed friction and restricted by the coast shape this wave moves towards Jianggang in the shape of an arc with Jianggang at the center of the arc at a speed of 100 km per hour (fig. 2). Controlled by this special tidal wave,

## 1 A basic hydraulic factor of forming and maintaining the radial sand ridges—tidal current controlled by the moving stationary tidal wave

Many researchers have shown interest in the impact of the distribution of tidal wave and tidal current on the radial sand ridges for a long time. In the 1980s, based on the measured data from the comprehensive survey of the China coast, combined with some numerical tidal wave results, some investigators suggested that there were two different tidal wave systems meeting outside Jianggang, and the strong tidal currents of these tidal wave systems induced the evolution of the sand ridges and were a major factor of the radial plane form<sup>[1-4]</sup>. The authors consider that to deepen the study on this matter, three questions must be answered. Firstly, can the present tidal current field build and maintain the radial plane form and the vertical shape of wide shoals and deep troughs? Secondly, in the early days of the sand ridge development, could the tidal current field provide basic hy-

flood currents surge towards Jianggang from various directions of north, northeast, east and southeast, while ebb currents disperse in a 150-degree-fan-shape taking Jianggang as the center. As a result, the unusual large tide range appears near Jianggang and the radial current forms (fig. 3). Therefore, the stationary wave character, the large tide range and the radial tidal current field are the characteristics of currents over the area.

Through a careful analysis of fig. 3, it is found that the radial sand ridge area can be divided into two stretches by a line between Jianggang and Huangshayang, namely the southern stretch and the northern stretch. In the southern stretch, the

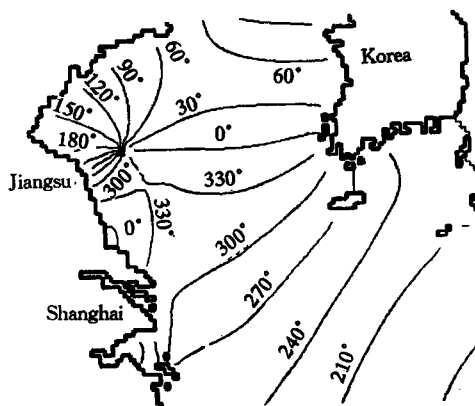


Fig. 2. Iso-phase lines of constituent  $M_2$ .

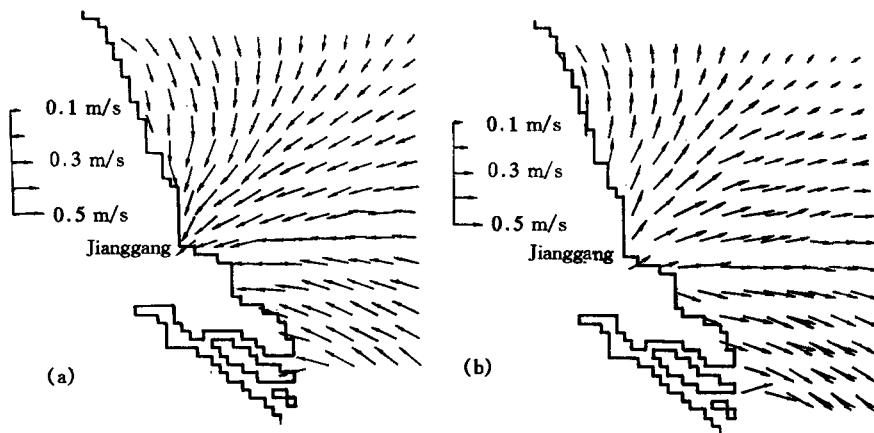


Fig. 3. Tide currents of constituent  $M_2$ . (a) Flood current; (b) ebb current.

dominant current direction of flood current and ebb current is SE-NW. The northern stretch can be subdivided into two parts, that is, the nearshore part and the offshore part. In the nearshore part the current is along the coast and in the direction of S-N. In the offshore part the current is radial current within a fan from northeast to southwest. The above results are fully consistent with the conclusions of profile shooting and sample analysis of Nanjing University<sup>1)</sup>, indicating that the plane form of the radial sand ridges is completely determined by the tidal current field.

The characteristics of stationary wave together with the large tide range result in the peculiar radial plane distribution of sand ridges and the wide-shoal-deep-channel relief. In a stationary wave, the current velocity reaches the maximum value at the half tidal level. At the half flood tidal level, strong currents suspend bed materials and make the sediment concentration maximum. After the half tidal level, with the rising of tidal level, the current velocity becomes weaker and weaker, and the sand-carrying capacity becomes lower and lower; thus sediments gradually deposit. During the spring tide, owing to the contribution of the large tidal range sediments move

1) Wang Ying, Zhu Dakui, Zhou Lufu et al., *Morphology and Depositional Characters and Evolution Pattern of the Radial Sand Ridges Over the Yellow Sea Seafloor*, report of project supported by the National Natural Science Foundation of China, 1998.

towards the coast and form a vast flat floodplain; during the neap tide sediments move a shorter distance. During the ebb tide, water over the floodplain rushes into channels and causes strong erosion. The vertical shape of wide-shoal-deep-channel is closely related to the tide characteristics of the area.

### 1.2 Old tidal current field and palaeo-Yangtze River underwater accumulation

By profile shooting and sample analysis it is found that there exists a palaeo-river in the southern part of the radial sand ridges, which provides the basis for the argument that the radial sand ridges are developed from the palaeo-Yangtze River underwater accumulation<sup>1)</sup>. Then, questions arise. What is the dynamic mechanism of the palaeo-Yangtze River underwater accumulation? Does it have a certain connection with the present dynamic environment over the area? The results of simulated tidal currents answer these two questions.

The old current field and the present current field are generally the same. However, obvious differences exist in the vicinity of the palaeo-river estuary; that is, there is a convergent-divergent tidal zone 100 km away from the estuary. Because of tidal lag, the flood current from the ocean meets the ebb current from the river, then convergence happens (fig. 4(a)). For the same reason, divergence appears (fig. 4(b)). It is not difficult to understand that the palaeo-river estuary is a bay. The tidal wave in the bay has the character of stationary wave. The wave node and wave loop are at the mouth and the top of the bay respectively. During the flood tide period, water surges towards the shore and emerges with the ebb current from the river, forming an arcshaped tidal convergent zone. This zone is in another opposite wave loop.

"The old current field" shows a convergent-divergent tidal zone in the vicinity of the palaeo-Yangtze River estuary. This zone provides a dynamic environment for the formation of the palaeo-

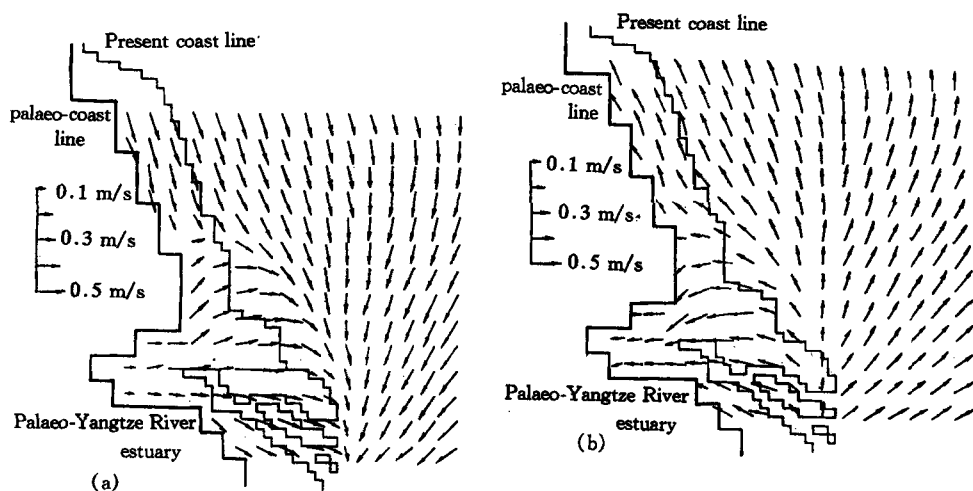


Fig. 4. Tidal currents of constituent  $M_2$  in the palaeo-river estuary. (a) Ebb tide in the inner part; (b) flood tide in the inner part.

1) Wang Ying, Zhu Dakui, Zhou Lufu et al., *Morphology and Depositional Characters and Evolution Pattern of the Radial Sand Ridges Over the Yellow Sea Seafloor*, report of project supported by the National Natural Science Foundation of China, 1998.

estuary delta. During the period of ebb tide, sediments in the river move towards the mouth with river runoff, and are stopped by the flood current from the sea in the vicinity of the convergent-divergent zone. At the same time the current velocity in the river becomes weaker and weaker; thus sediments gradually deposit. When ebb tide takes place outside the river mouth, flood tide takes place in the river, and some deposited sediments are picked up and carried towards the upper reaches. They meet sediments from the upper reaches; as a result, the sediment concentration is increased. In this dynamic environment sediments move back and forth between the top of the estuary and the convergent-divergent zone, gradually depositing and forming the palaeo-Yangtze River tide delta. The fine line in fig. 4 indicates the present coastal line. From the figure it can be seen that the present Nantong city is located in the palaeo-convergent-divergent tidal zone.

### 1.3 Old current field and present current field

Now that the old current field provided the dynamic environment for the formation of the palaeo-Yangtze delta, and the present current field has a dynamic character which helps with the formation of the radial sand ridges, the question is what the connection is between these two fields. Fig. 5 shows the iso-tide-phase lines of constituent  $M_2$  in the palaeo-coast profile. A comparison between fig. 2 and fig. 5 shows that the tidal wave distributions in the two figures are in very good agreement. In the two figures, the 330-degree iso-tide-phase lines almost overlap, indicating that the moving stationary tide wave over the sand ridge area existed in the palaeo-Yangtze River time, i. e. the moving stationary tidal wave over the sand ridges has been extremely stable.

It neither shifts with the evolution of the sand ridges nor changes with time. The moving stationary tidal wave in the palaeo-estuary controls the whole process from the formation to the development of the sand ridges. The causes of unchangeable tidal wave can be explained as follows: The moving stationary tidal wave over the sand ridges is the combination of the anticlockwise rotary tidal wave to the south of Shandong Peninsula and the following Yellow Sea progressive tidal wave. When the tidal waves from the East China Sea propagate towards the north Yellow Sea, some of the waves are stopped by the peninsula, forming anticlockwise rotary tidal waves, which will certainly converge with the following progressive waves, i. e. the tidal wave system covering the Yellow Sea is an inevitable outcome of ocean tidal wave propagation bounded by Korean Peninsula, Shandong Peninsula and the coast line of Jiangsu Province. Local variation of the coast line will not cause essential changes in this wave system.

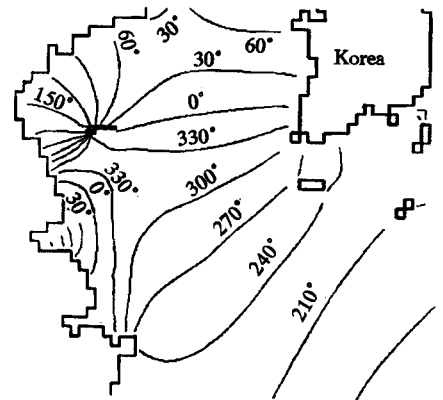


Fig. 5. Iso-phase lines of constituent  $M_2$  in palaeo-coast profile.

## 2 Functions of waves: local and conditional

As is known, nearshore wave action is one of the important factors causing coastal evolution. In the discussion on hydrodynamics over the sand ridge area, it is inevitable to consider wave distribution. However, over the wide sand ridge area, the tidal floodplain is wide, and the ridges and troughs are distributed alternatively. It is very difficult to use a conventional refraction

method for the computation of wave refraction effects. Conventional wave refraction diagrams in common use are suitable for the situation of regular seafloor relief. When underwater topography becomes complicated, like the radial sand ridge area, conventional wave refraction models meet difficulty. It is shown that these problems are often associated with the appearance of numerous caustics, and that numerical simulation cannot be carried out smoothly. To avoid the mentioned difficulties, a reverse-ray-path spectrum refraction model has been employed in this paper to determine the wave heights at different locations<sup>[8,9]</sup>.

### 2.1 Wave ray paths over the area

To understand the whole situation of wave distribution, the wave heights at 25 points over the sand ridge area are calculated. These 25 points are scattered all over the troughs (fig. 6). The possible wave ray paths to reach these points are simulated showing that a wave ray path depends upon the bed topography, the tidal level and the incident wave period.

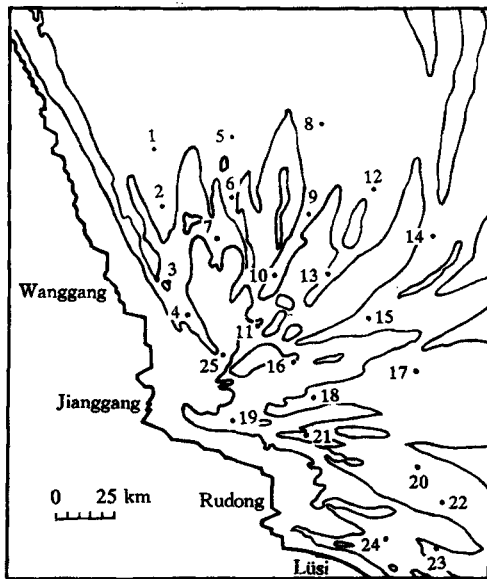


Fig. 6. Layout of 25 calculation points.

A comparison of fig. 7(a)—(c) shows that for point 3, only at the high tidal level can the long-period incident waves from NNE to SE approach point 3 while at a tidal level lower than the mean level incident waves from E and SE cannot reach the point. At that time waves from N or nearby can only reach the point by the Xiyang trough. That means that only at the high tidal level the wave impacts are overall, and when the tidal level is lower than the mean level, the wave impacts are local.

### 2.2 Wave height distribution under normal conditions

The averaged annual maximum wind speed over the sand ridge area is 17.74 m/s, and the corresponding significant incident wave height in offshore boundaries is 2.64 m which can be taken as the value for normal conditions.

Table 1 lists the simulated wave heights at 25 points by use of the reverse-ray-path spectrum refraction model. From the table the following can be found.

1) Under the condition of averaged annual maximum wind speed, the wave heights over the

depends upon the bed topography, the tidal level and the incident wave period. Take point 3 located in Xiyang as an example. At the high tidal level (2.98 m, abandoned Yellow River datum) short-period waves can reach the point within a 150-degree fan from northwest to southeast. With the increasing wave period, except for the waves from N and NNW, which are parallel to Xiyang, the paths from other directions are deflected and the wave ray paths which can reach point 3 become fewer and fewer (fig. 7(a)). At the mean tidal level (0.53 m), only short-period waves can reach the point within a 60-degree fan. For the wave period of 8 s the ray paths are obviously few and directions deflected (fig. 7 (b)). At the low tidal level (-1.92 m), the effects of seabed topography on ray paths are very obvious, and long-period waves can only approach point 3 by the Xiyang trough (figure 7(c)).

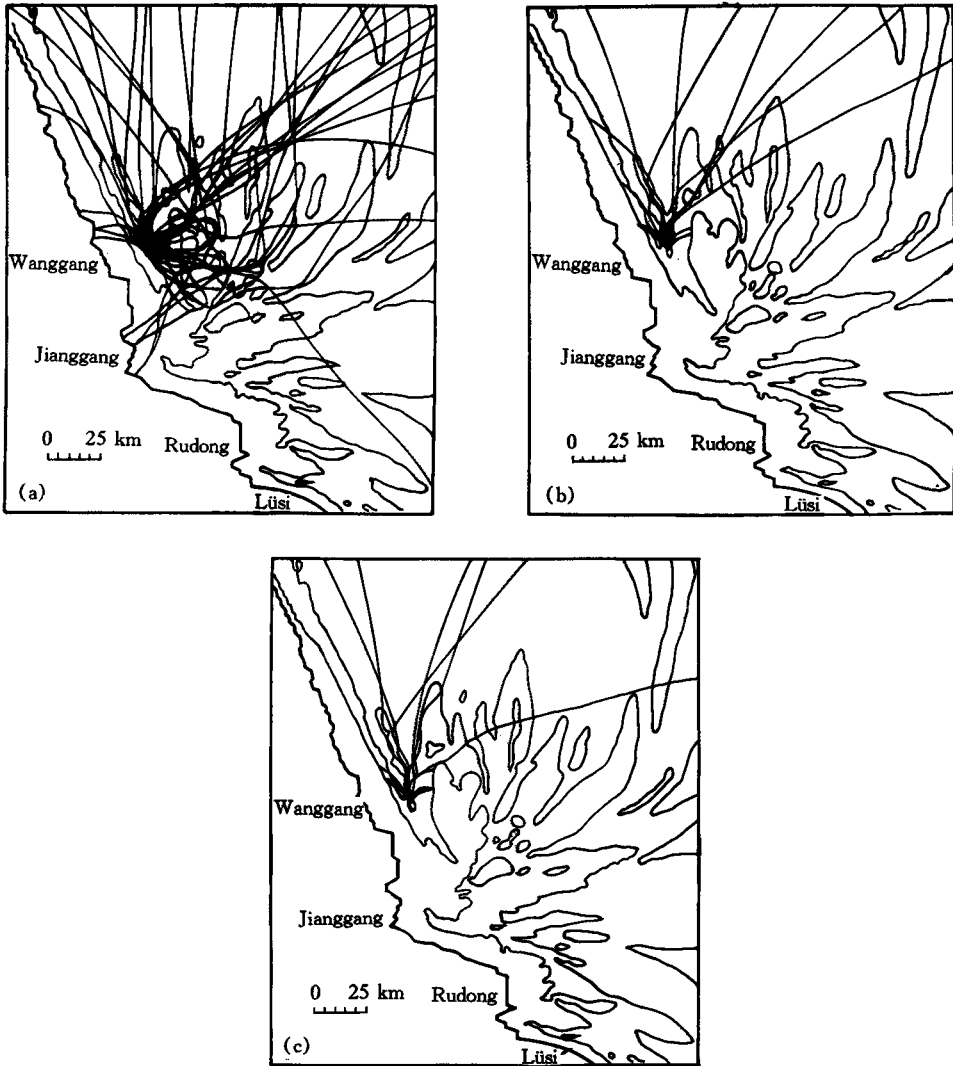


Fig. 7. Wave ray paths reaching point 3. (a) High water level; (b) mean water level; (c) low water level.

sand ridge area are small.

2) For every trough, the wave height at the nearshore end is larger than the wave height at the offshore end.

3) The radial sand ridge area can be divided into two stretches by a line between Jianggang and Huangshayang, namely the southern stretch and the northern stretch. In the northern stretch, the height of wave from NE is larger than that from SE, while the height of wave from ESE is larger than that from NE in the southern stretch.

4) Affected by the seabed topography, the wave height at Xiyang is small. However, because of the wide water area, the wave heights at Caomushuyang, Kushuiyang, Huangshayang and Lanshayang are large.

Table 1 Wave heights at averaged annual maximum wind speed (17.74 m/s)

Water area	Point No.	NE			ESE		
		high water level	mean water level	low water level	high water level	mean water level	low water level
Xiyang	1	2.53	2.48	2.45	1.99	1.88	1.81
	2	2.38	2.25	2.02	1.94	1.76	1.43
	3	1.75	1.22	0.85	1.10	0.77	0.50
	4	1.10	0.44	0.33	0.88	0.27	0.17
	25	1.91	0.00	0.00	1.91	0.00	0.00
Xiaobeicao	5	2.65	2.59	2.61	2.44	2.37	2.33
	6	2.49	2.36	2.32	2.60	2.62	2.58
	7	2.56	2.63	2.56	1.73	1.39	1.39
Chenjiawucao	8	2.59	2.57	2.57	2.51	2.44	2.42
	9	2.61	2.61	2.71	2.64	2.67	2.67
	10	2.70	2.28	2.02	2.60	2.32	1.89
	11	2.01	0.61	0.41	1.58	0.38	0.27
Caomushuyang	12	2.64	2.54	2.58	2.76	2.68	2.68
	13	2.57	2.46	2.57	2.52	2.41	2.21
Kushuiyang	14	2.51	2.42	2.40	2.74	2.74	2.80
	15	2.61	2.45	2.58	2.58	2.52	2.54
	16	2.39	2.25	2.17	2.43	2.09	1.97
Huangshayang	17	2.65	2.56	2.53	2.57	2.52	2.52
	18	2.64	2.55	2.46	2.25	2.02	2.03
Xiaoyanggang	19	1.68	1.10	0.68	1.57	1.05	0.71
	20	2.58	2.51	2.50	2.53	2.45	2.45
Lanshayang	21	2.22	1.88	1.68	2.23	2.18	1.99
	22	2.62	2.57	2.51	2.50	2.44	2.40
Xiaomiaohong	23	2.77	2.80	2.85	2.43	2.37	2.30
	24	2.19	1.94	1.77	2.50	2.50	2.38

5) There exists a calm area around Jianggang (points 4, 11, 19, and 25) of about 50 km<sup>2</sup>. Under normal conditions the wave height is smaller than 1 m.

6) In shallow water areas, the wave heights at different water levels are very different. For point 4, the wave heights at the high level, mean level and low level are 1.10, 0.44 and 0.33 m, respectively. For point 25, the wave height is 1.91 m at the high water level, and when the water level is lower than the mean level, the wave height is equal to zero.

It should be pointed out that the values in table 1 are corresponding to the averaged annual maximum wind speed. Wind speeds under normal weather conditions are lower than the averaged annual maximum wind speed, so the wave heights are smaller than the values in the table.

### 2.3 Wave height distribution under storms

To obtain the wave height distribution under storms the 25-year-return-period wind speed (26.7 m/s) from NE and ESE are used to estimate the wave height over the area. Table 2 lists the results.

Table 2 shows the following points.

1) During the period of high tidal level, the wave heights at most points are larger than 4.0 m except for a few points in Xiyang.



Table 2 Wave heights at 25-year-return-period wind speed (26.7 m/s)

Water area	Point No.	NE			ESE		
		high water level	mean water level	low water level	high water level	mean water level	low water level
Xiyang	1	5.15	5.08	4.95	3.98	3.75	3.61
	2	4.80	4.57	4.02	3.90	3.50	2.70
	3	3.14	2.33	1.40	1.96	1.49	0.80
	4	1.71	0.80	0.48	1.26	0.51	0.25
	25	2.08	0.00	0.00	2.08	0.00	0.00
Xiaobeicao	5	5.39	5.30	5.07	4.99	4.78	4.67
	6	5.01	4.74	4.58	5.28	5.34	5.04
	7	3.94	3.44	2.84	3.36	2.73	2.61
Chenjiawucao	8	5.31	5.28	5.24	5.08	4.94	4.85
	9	5.28	5.30	4.99	5.38	5.35	4.99
	10	5.34	4.54	3.67	5.15	4.53	3.48
	11	3.50	1.18	0.77	2.76	0.73	0.48
Caomushuyang	12	5.36	5.18	4.81	5.53	5.18	4.81
	13	5.13	5.05	5.01	5.09	4.91	4.41
Kushuiyang	14	5.05	4.92	4.87	5.66	5.69	5.66
	15	5.17	4.95	4.98	5.28	5.20	4.98
	16	4.79	4.51	4.09	4.77	4.14	3.69
Huangshayang	17	5.34	5.19	5.10	5.25	5.18	5.14
	18	5.27	5.05	4.64	4.50	4.08	4.00
Xiaoyanggang	19	3.17	2.07	1.11	3.13	2.04	1.12
Lanshayang	20	5.25	5.14	5.08	5.17	5.06	5.03
	21	4.31	3.69	3.25	4.52	4.42	3.87
	22	5.36	5.24	5.13	5.12	5.01	4.89
Xiaomiaohong	23	5.45	5.09	4.71	4.99	4.84	4.70
	24	4.42	3.96	3.43	4.71	4.30	3.84

2) The wave heights at troughs between shoals are obviously small and very different with the directions. For example, at point 7 the waves from NE and ESE are 3.94 and 3.36 m for the high water level, and 3.44 and 2.73 m, respectively, for the mean water level.

3) With the decrease of water level the wave heights at troughs decrease rapidly. For example, the wave heights, at point 11, are 2.76, 0.73 and 0.48 m for the high, mean and low water levels, respectively. However, the wave heights at the edges of the sand ridges are less influenced by the water level. For instance, the wave heights at point 8 are 5.31 and 5.24 m for the high and low water levels, respectively.

#### 2.4 Effect of waves on morphological evolution of sand ridges

Computational results of the wave field over the area show that under the condition of averaged annual maximum wind speed, the wave height is about 2 m. When the water level is below the mean water level, waves are smaller. Moreover, the wave heights at different positions are very different. The authors consider that the waves under normal conditions only have an impact on the micro-morphology. On the macro-morphology of either the plane form or the vertical shape, their impact is in the lower scale than that of tidal currents.

Under the condition of 25-year-return-period wind speed and at the high water level, the

wave height is about 4 m. The corresponding wind speed and scale are 26.7 m/s and 10, respectively. Therefore, it can be thought that under the condition of typhoon or cold wind, waves can have a significant influence on the seabed topography.

### 3 Combined action of storm surge and storm current recovery of the sand ridge topography

The sand ridge area is often attacked by storm surges. Storm surge and storm current are two different aspects of the storm disaster. The characters of storm current are of wide scope, high velocity and changeable direction. Storm current is very dangerous to ships in navigation and coastal structures, and what is more, its impact on nearshore bed topography is much stronger than that of the normal tidal current.

#### 3.1 Simulation results of storm current

The storm current field induced by typhoon is a huge anticlockwise vortex. The center of vortex and the center of typhoon are not in the same position; there is a little deviation. A vortex can cover 4 latitudes (about 400 km). The vortex center, current velocity and current direction change with the path, moving speed, and the strength of the typhoon. A numerical model simulating the typhoon process covering the whole East China Sea was established using the embedded grid system to track the typhoon path and to finely simulate the nearshore seafloor relief<sup>[10]</sup>.

Three kinds of typhoons have influence on the Jiangsu coast: They are typhoons moving northwards on the sea, typhoons landing on the Yangtze River estuary and typhoons turning away on the sea. Calculation and analysis show that among the three the latter two could have significant influences on the radial sand ridge area. The simulation results of typhoon No. 7708, which landed on the Yangtze River estuary, and typhoon No. 8114, which turned away on the sea, show that both could cause 2-m storm surge near Lüsü. Before they landed or turned away, the vortex center was located to the southeast of the Yangtze River estuary and the vortex covered the whole radial sand ridge area. The currents in the area are a part of the anticlockwise vortex, and the current directions are basically parallel to the coast line from north to south. The magnitude of

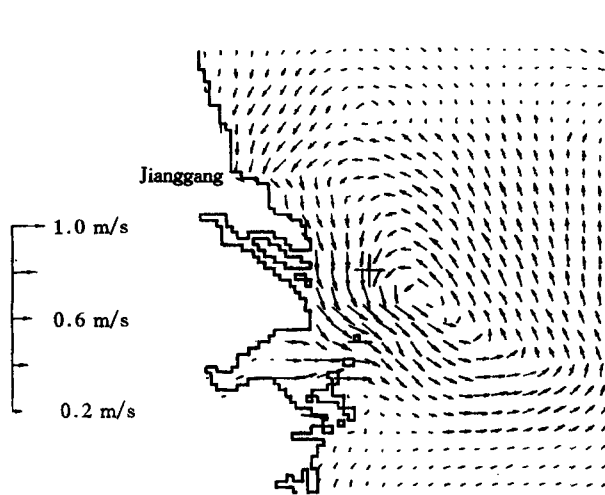


Fig. 8. Storm currents during the period of typhoon No. 7708 (2 am, September 11, 1997).

a current can reach 1 m/s. Taking the line between Jianggang and Dongshayang as a boundary, the angle between the current direction and the ridge-channel/trough in the northern part of the area is smaller than that in the southern part where the current direction may even be perpendicular to the ridge-channel/trough. Fig. 8 shows the storm current field of typhoon No. 7708 at 2 o'clock, September 11, 1977. At that time the typhoon center was 70 km away east of Chongming Island. The huge anticlockwise vortex controlled a very wide area from Hangzhou Bay of Zhejiang Province to Sheyang estuary of Jiangsu Province.

### 3.2 Storm current and typhoon wave are major factors causing short-term changes of radial sand ridges

Computational results of the wave field over the radial sand ridge area show that under the condition of average annual maximum wind speed, the wave height is about 2 m, and there exist quite obvious differences for different locations. Under this condition, the influence of waves on the sand ridges is not significant. Under the condition of 25-year-return-period wind speed and at the high water level, the wave height is about 4 m, and the wave distribution is relatively even. There exist some impacts on the sand ridges over the whole radial sand ridge area.

The causes of storm currents are different from those of tidal currents. Therefore, their patterns of distribution and change have their own special characters. If the periodic change of magnitude and direction is taken as the character of tidal current, the random change is the character of storm surge.

In the study of coast and estuary evolution, a commonly used concept is sediment carrying capacity. Some researches have been conducted on the sediment carrying capacity under the combined action of waves and tidal currents, and a few formulae are obtained. Although those formulae are in different forms, the sediment carrying capacity in those formulae is directly proportional to a certain power of current velocity and wave height. When a typhoon strikes the radial sand ridge area, the water level rises 1—2 m, the wave height can reach 4 m, and the storm current can reach 1 m/s or so. Such a strong dynamic condition can certainly induce a much higher sediment carrying capacity than normal tidal currents. This will have a tremendous impact on the relatively stable bed topography. Unlike the tidal current direction along the channels/troughs between ridges, the storm current direction is oblique to sand ridges and channels/troughs. The result is that ridges and shoals suffer heavy erosion, and the eroded materials enter channels/troughs causing deposition. Although further researches on the mechanism of sediment suspension and deposition during a storm are necessary, the pattern of shoal-erosion and channel/trough-deposition during a storm has been proved by some measured data. In the early 1980s, after the attack of typhoon No. 8114, a significant change of topography in the Taiyang shoal of the sand ridges is one of the proofs.

A storm lasts, after all, only a short time. After the storm, the tidal current becomes a dominant factor again. Under the tidal action, the underwater topography will gradually return to its "original shape". "Tidal current-induced formation"—"storm-induced change"—"tidal current-induced recovery" is the evolution pattern of the contemporary sand ridges. However, it should be pointed out that (i) the process of remake of sand ridges by tidal currents is a gradual process and the final result is not exactly the original shape but a similar one. After several circles, the displacements of ridges and channels/troughs as well as the changes of bed topography will take place; (ii) from the point of view of geomorphology, under the tidal action the radial sand ridges are stable, but from the point of view of engineering the changes caused by storm are significant, even tremendous. Close attention should be paid to the feasibility study of coastal engineering projects in this area.

## 4 Conclusions

1) Tidal current is the major hydraulic factor inducing the formation and maintenance of the radial sand ridges. The characteristics of stationary wave together with the large tide range and

radial tidal current field result in the peculiar radial plane distribution of sand ridges and the wide-shoal-deep-channel/trough relief.

2) The presence of Korean Peninsula, Shandong Peninsula and Jiangsu coast determines the inevitability of the convergent tidal wave system along Jiangsu coast. The moving stationary tidal wave supplies a necessary dynamic environmental condition not only for the palaeo-Yangtze River underwater delta in the old days but also for the formation and maintenance of the radial sand ridges in the present days.

3) The palaeo-Yangtze River underwater delta is the base of the radial sand ridges. The sediment of the present sand ridges comes from the palaeo-Yellow River estuary and the Yangtze River.

4) Under normal conditions, the wave has little impact on the radial sand ridges. However, when there is a typhoon, the combined action of typhoon wave and storm current can have significant effects on the bed topography of the sand ridge area. The whole evolution process of the radial sand ridges takes a cycle which can be described as "storm-induced change—tidal current-induced restoration—storm-induced change again—tidal current-induced restoration" again. However, this process does not simply repeat itself. The local bed topography is obviously changed in this unclosed cycle.

## References

- 1 Li Chengzhi, Li Benchuan, Study on the cause of formation of underwater shoals along northern Jiangsu coast, *Oceanologica et Limnologia Sinica* (in Chinese), 1981, 12(4): 321.
- 2 Xia Dongxing, Liu Zhengxia, Formation mechanism and evolution condition of tidal current ridges, *Acta Oceanologica Sinica* (in Chinese), 1984, 6(3): 361.
- 3 Zhu Dakui, Fu Mingzuo, Preliminary study on the radial sand ridges along Jiangsu coast, in *Proceedings of Comprehensive Survey of Dongsha Shoal on the Jiangsu Coast* (in Chinese), Beijing: Ocean Press, 1986, 28—32.
- 4 Huang Yichang, Wang Wenqing, Research on the dynamic mechanism for radial sand ridges, *Acta Oceanologica Sinica* (in Chinese), 1987, 9(2): 209.
- 5 Zhao Baoren, Fan Guohong, Cao Deming, Numerical simulation of tides and tidal currents in the Bohai China Sea, the Yellow Sea and the East Sea, *Acta Oceanologica Sinica* (in Chinese), 1994, 16(5): 1.
- 6 Larsen, L. H., Cannon, G. A., Choi, B. H., East China Sea tidal current, *Continental Shelf Research*, 1985, 4: 77.
- 7 Zhang Dongsheng, Zhang Junlun,  $M_2$  tidal wave in the Yellow Sea radiate shoal region, *Journal of Hohai University* (in Chinese), 1996, 24(5): 35.
- 8 Shen Yujiang, Qian Chengchun. Interpretation of mechanism of semidiurnal tidal wave in the Yellow Sea, *Acta Oceanologica Sinica* (in Chinese), 1993, 15(6): 16.
- 9 Zhang Changkuan, Zhang Dongsheng, A model of wave refraction over the radiate shoal, *Journal of Hohai University* (in Chinese), 1997, 25(4): 1.
- 10 Zhang Junlun, Sheng Genming, Numerical model of Yangtze Estuary storm surge, *Journal of Hohai University* (in Chinese), 1987, 15(1): 8.